Gromet-Elhanan, Z. (1974) *J. Biol. Chem. 249*, 2522–2527.
Gromet-Elhanan, Z., & Khananshvili, D. (1984) *Biochemistry 23*, 1022–1028.
Gromet-Elhanan, Z., & Khananshvili, D. (1986) *Methods Enzymol. 126*, 528–538.
Grubmeyer, C., Cross, R., & Penefsky, H. S. (1982) *J. Biol. Chem. 257*, 12092–12100.
Harris, D. A. (1978) *Biochim. Biophys. Acta 463*, 245–273.
Hirano, M., Takeda, K., Kanazawa, H., & Futai, M. (1984) *Biochemistry 23*, 1652–1656.
Issartel, Y. P., & Vignais, P. V. (1984) *Biochemistry 23*, 6591–6595.
Kagawa, Y., Sone, N., Hirata, M., & Yoshida, M. (1979) *J. Bioenerg. Biomembr. 11*, 39–70.
Khananshvili, D., & Gromet-Elhanan, Z. (1982) *J. Biol. Chem. 257*, 11377–11383.
Khananshvili, D., & Gromet-Elhanan, Z. (1983) *J. Biol. Chem. 258*, 3714–3719.
Khananshvili, D., & Gromet-Elhanan, Z. (1984) *FEBS Lett. 178*, 10–14.
Khananshvili, D., & Gromet-Elhanan, Z. (1985a) *Biochemistry 24*, 2482–2487.
Khananshvili, D., & Gromet-Elhanan, Z. (1985b) *Proc. Natl. Acad. Sci. U.S.A. 82*, 1886–1890.
Lowry, O. H., Rosebrough, N. J., Farr, A. L., & Randall, R. J. (1951) *J. Biol. Chem. 193*, 265–275.
Nelson, N. (1981) *Curr. Top. Bioenerg. 11*, 1–35.
Ohta, S., Tsuboi, M., Oshima, T., Yoshida, M., & Kagawa, Y. (1980a) *J. Biochem. (Tokyo) 87*, 1609–1617.
Ohta, S., Tsuboi, M., Yoshida, M., & Kagawa, Y. (1980b) *Biochemistry 19*, 2160–2165.
O'Neal, C. C., & Boyer, P. D. (1984) *J. Biol. Chem. 259*, 5761–5767.
Penefsky, H. S. (1977) *J. Biol. Chem. 252*, 2891–2899.
Penefsky, H. S. (1979) *Adv. Enzymol. Relat. Areas Mol. Biol. 49*, 223–280.
Philosoph, S., Binder, A., & Gromet-Elhanan, Z. (1977) *J. Biol. Chem. 252*, 8747–8752.
Senda, M., Kanazawa, H., Tsuchiya, T., & Futai, M. (1983) *Arch. Biochem. Biophys. 220*, 398–404.
Senior, A. E., & Wise, J. G. (1983) *J. Membr. Biol. 73*, 105–124.
Senter, P., Eckstein, F., & Kagawa, Y. (1983) *Biochemistry 22*, 5514–5518.
Stan-Lotter, H., & Bragg, P. D. (1984) *Biochem. J. 224*, 145–151.
Steitz, T. A., Harrison, R., Weber, I. T., & Leahy, M. (1982) in *Mobility and Function in Proteins and Nucleic Acids*, Ciba Foundation Symposium 93, pp 25–46, Pitman, London.
Weber, M., & Osborn, U. (1969) *J. Biol. Chem. 244*, 4406–4412.
Wieker, H. J., & Hess, B. (1985) *Biochim. Biophys. Acta 806*, 35–41.
Yoshida, M., Sone, N., Hirata, H., & Kagawa, Y. (1977) *J. Biol. Chem. 252*, 3480–3485.

Anomalous Oxygen-18 Exchange during ATP Synthesis in Oxidative Phosphorylation†

Jacqueline J. Sines and David D. Hackney*
Department of Biological Sciences, Carnegie-Mellon University, Pittsburgh, Pennsylvania 15213
Received April 2, 1986; Revised Manuscript Received May 8, 1986

ABSTRACT: The synthesis of ATP from highly enriched [^{18}O]P_i by submitochondrial particles driven by succinate oxidation produces distributions of ^{18}O-labeled ATP species that deviate from the distributions predicted by a simple model for the exchange. Control experiments indicate no change in isotopic distribution when [^{18}O]ATP is synthesized from [^{18}O]ADP by adenylate kinase, which is bound to the submitochondrial particles. The observed deviations are in the opposite direction from that produced by heterogeneity due to multiple pathways for ATP synthesis. Two types of complex models can account for the observed deviations. One model has nonequivalence of the P_i oxygens during the exchange reaction, due to incomplete randomization of the P_i oxygens during the reversible cycles of hydrolysis and synthesis of bound ATP. The other model assumes that, during each turnover, a slow transition must occur between a high-exchange and a low-exchange pathway.

Analysis of the exchange reactions of labeled oxygen atoms between water and phosphate has proven to be an important probe of the mechanisms of a number of enzymes that synthesize or hydrolyze phosphoesters. [See Mitchell (1984) for a recent review.] The simple synthesis model of Scheme I illustrates the probable source of the multiple water oxygens often observed in the products of such reactions. If ATP is synthesized in unenriched water from P_i that has all four

Scheme I

$$E + ADP + P_i \underset{k_{-1}}{\overset{k_1}{\rightleftharpoons}} E{\cdot}ADP{\cdot}P_i \overset{HOH}{\underset{k_{-2}}{\overset{k_2}{\rightleftharpoons}}} E{\cdot}ATP \underset{k_{-3}}{\overset{k_3}{\rightleftharpoons}} E + ATP$$

oxygens labeled with ^{18}O, then the product will have three ^{18}O-labeled oxygens if $k_{-2} \ll k_3$. However, if $k_{-2} \gg k_3$, then many reversals of step 2 will occur before product release, and most of the ^{18}O label will be lost if the bound phosphate is capable of randomizing its oxygens between reversals. Thus, a model based on nonrestrictive phosphate binding, coupled with a product release rate that is slow in comparison to reaction reversal, predicts extensive oxygen exchange. Most

†Supported by Grant AM25980 and Predoctoral Training Grant GM08067 (to J.J.S.) from the U.S. Public Health Service and an Established Investigatorship from the American Heart Association (to D.D.H.). Preliminary work has been reported (Hackney, 1983).

0006-2960/86/0425-6144$01.50/0

previous theoretical treatments have assumed that the bound P_i has sufficient rotational freedom to allow complete scrambling of its four oxygens between reversals of step 2. The further assumption of a single enzymatic pathway allows an estimation of the relative values of k_3 and k_{-2} on the basis of the average ^{18}O enrichment of product. A detailed theoretical treatment of this model that predicts the complete distribution of labeled product containing zero to three ^{18}O oxygens in the ATP has been presented (Hackney, 1980; Hackney et al., 1980).

Deviations from predicted distributions can provide information about where this simple model breaks down. Heterogeneity in the reaction (e.g., multiple pathways, each following a simple random mechanism, but with different relative values of k_{-2} and k_3) would be indicated by distributions in which $^{18}O_0$ and $^{18}O_3$ species are elevated with respect to distributions for a single pathway at the same average enrichment. A corresponding deficit would occur for the observed $^{18}O_1$ and $^{18}O_2$ species. Distributions that deviate in this direction from those predicted by a simple model will be refered to as end weighted. Previous work (Hackney, 1984) with ATP synthesis by oxidative phosphorylation had indicated that the oxygen exchange that was observed could be approximately described by a simple model. Small deviations were noted, however, particularly at low ADP levels, and the observed deviations were biased in favor of the singly and doubly labeled species (center weighted) in contrast to the case with heterogeneity. This paper presents a careful determination of the distribution of [^{18}O]ATP species obtained by synthesis at low ADP, along with control experiments indicating that the observed deviations are significant. It is further demonstrated that such center-weighted deviations can be produced by two types of complex models involving either nonequivalence of the P_i oxygens or a slow interconversion between alternate reaction pathways.

Nonequivalence of the P_i oxygens has been suggested (Shukla & Levy, 1977a,b) as the basis for the reduced amount of oxygen exchange observed in ATP hydrolysis by myosin relative to that predicted on the basis of transient kinetic experiments. One of the initial applications of the analysis of the distribution of ^{18}O-labeled species was the demonstration (Sleep et al., 1980; Shukla et al., 1980; Midelford, 1981; Hackney, 1982) that such nonequivalence did not occur with myosin but that the decrease exchange was due to heterogeneity in hydrolysis pathways. No evidence for nonequivalence of P_i oxygens has been obtained up to now in any of the cases where distribution data are available, as discussed previously (Hackney, 1980). At the β-phosphoryl position of ATP, however, incomplete positional isotopic exchange has been observed during medium ATP–HOH exchange by chloroplast (Wimmer & Rose, 1977) and myosin (Geeves et al., 1980). One possible explanation for this incomplete exchange is that it results from incomplete scrambling of the oxygens on the ADP between reversals of the hydrolytic step [see Rose (1979) for review].

Experimental Procedures

Beef heart mitochondrial preparations (Hackney & Boyer, 1978) and general methods for analysis of the ^{18}O exchange reaction (Hackney et al., 1980) were as previously described. Hexokinase, glucose-6-phosphate dehydrogenase, and soluble adenylate kinase were obtained from Sigma Chemical Co. and dialyzed before use.

Exchange Reactions. The reaction mixture at pH 7.6 and 30 °C consisted of 50 mM sucrose, 50 mM glucose, 50 mM Hepes[1] /KOH, 25 mM sodium succinate, 10 mM $MgCl_2$, 25 mM KCl, 10 mM AMP, 40–85 units/mL hexokinase, submitochondrial particles at 0.37–0.40 mg/mL, ADP, and 15 mM [^{18}O]P_i. The complete mix minus P_i and ADP was incubated for 4 min before initiation of the exchange reaction by sequential addition of ADP and P_i. The reaction was quenched with addition of a half-volume of cold 2 N perchloric acid, and nucleotides were removed by adsorption on charcoal. The supernatant following centrifugation was neutralized with KOH, the $KClO_4$ precipitate removed by centrifugation, and the supernatant purified by anion-exchange chromatography (Hackney et al., 1980). The P_i and G6P were eluted with 30 mM HCl, lyophilized, and dissolved in a minimal volume, and the G6P was oxidized to 6PG with NADP and glucose-6-phosphate dehydrogenase (Hackney et al., 1979). ^{31}P NMR spectra were obtained at 121 MHz on a Bruker HX300 with broad-band proton decoupling and D_2O as an internal lock.

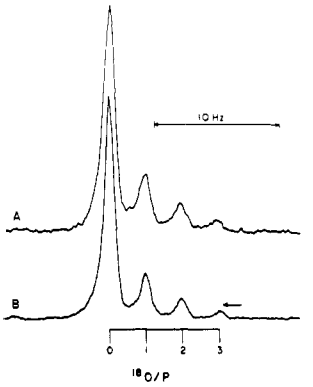

FIGURE 1: ^{31}P NMR of [^{18}O]-6-phosphogluconate. ATP was synthesized from ADP and [^{18}O]P_i by submitochondrial particles at 20 and 10 μM ADP for A and B, respectively, and converted to 6-phosphogluconate.

Results

Intermediate Exchange during ATP Synthesis at Low ADP. ATP was synthesized from ADP and highly enriched [^{18}O]P_i by submitochondrial particles driven by succinate oxidation. Hexokinase and glucose were present to trap the ATP as G6P and regenerate ADP. AMP was usually included to inhibit adenylate kinase. The trapping of ATP inhibits the flux of both the back-hydrolysis of free ATP and the release of P_i back to the medium via reversal of step 1 after it has entered the exchange cycle (Hackney & Boyer, 1978). The G6P and P_i were isolated together, and G6P was converted to 6PG for NMR analysis of its ^{18}O isotopic composition (Hackney et al., 1979). Figure 1 presents the high-resolution ^{31}P NMR spectrum obtained for 6PG produced at ADP concentrations of 10 and 20 μM and Table I contains the quantitation of the distributions for both the P_i and the 6PG. The P_i contained mainly the species with four ^{18}O, and the predominance of the 6PG species with no ^{18}O indicates that most of the isotope was exchanged out during ATP synthesis and replaced with ^{16}O derived from the unenriched water pool. Such extensive exchange is expected at low ADP concentrations (Hackney & Boyer, 1978; Hackney, 1984) and would be produced by an average of 29 and 23 reversals of step 2 during each net turnover at 10 and 20 μM ADP assuming a simple random model. This corresponds to P_c values [$k_{-2}/(k_{-2} + k_3)$] of 0.967 and 0.958, respectively.

Although the absolute deviations are not large between the experimental and theoretical distributions, the relative amounts

[1] Abbreviations: G6P, glucose 6-phosphate; 6PG, 6-phosphogluconate; Hepes, 4-(2-hydroxyethyl)-1-piperazineethanesulfonic acid.

Table I: Distributions of Isotopic ^{18}O Species

ADP (μM)		$^{18}O_0$	$^{18}O_1$	$^{18}O_2$	$^{18}O_3$	$^{18}O_4$
10	P_i[a]	1.0	0.2	0.7	9.4	88.7
	ATP obsd[b]	76.8	14.1	6.6	2.5	
	theory					
	simple	79.2	10.7	6.1	4.0	
	nonequivalent[c]	76.9	14.0	6.6	2.5	
	square[d]	76.4	14.4	6.6	2.6	
20	P_i[a]	1.1	0	0.7	9.4	88.8
	ATP obsd[b]	71.8	16.4	8.5	3.3	
	theory					
	simple	74.4	12.9	7.6	5.1	
	nonequivalent[c]	71.5	16.9	8.4	3.2	
	square[d]	73.8	15.1	7.7	3.4	

[a] P_i distribution is average of initial and final P_i distributions. [b] Corrected for natural abundance of ^{18}O by transfer of 0.8% of $^{18}O_0$ from $^{18}O_1$ to $^{18}O_0$. [c] Nonequivalent model calculated for subsite interaction energies of 5.5/9/5.5/5.5 kcal/mol with one favored 2-fold rotation at 10^8 s^{-1} and with k_1P_i, k_{-1}, k_2, k_3, k_{-3}, and k_{ATP} values of 10^4, 0, 10^3, 10, 0, and 0 s^{-1}, respectively. Rotational rate constants of k_A, k_C, and k_D were 1.36×10^{-2} s^{-1}; k_B was 5.0 s^{-1}; k_{AB} and k_{AC} were 1.27×10^{-6} s^{-1}; k_{AD} was 6.0 s^{-1}. For 10 and 20 μM ADP, the k_{-2} values were 1.65×10^4 and 1.3×10^4 s^{-1}, respectively. See supplementary material for details. [d] Square model calculated for Scheme II with $k_1 = k_{-e} = k_2 = k_{-2} = k'_2 = k'_{-2} = 400$ s^{-1}; $k_a = k_p = 22$ s^{-1}; $k'_3 = 20$ s^{-1}; all other rate constants are equal to zero.

of the higher enrichment species do differ significantly. For example, the observed ratio of the $^{18}O_3/^{18}O_2$ species of less than 0.4 is particularly striking in view of the fact that a simple random model predicts a limiting lower value at infinite exchange of 0.62 for ATP synthesis from the P_i that was used in this experiment. Intuitively, it might be expected that the $^{18}O_3/^{18}O_2$ ratio should approach zero in the limit of high exchange (i.e., as k_{-2}/k_3 approaches infinity), but this is not the case. Limiting ratios at high exchange of 2/3 for $^{18}O_3/^{18}O_2$ and 1/2 for $^{18}O_2/^{18}O_1$ are in fact predicted by a simple random model assuming 100% enrichment in the starting P_i. With increasing extents of exchange, the amounts of the $^{18}O_1$, $^{18}O_2$, and $^{18}O_3$ species in the released ATP decrease with respect to the $^{18}O_0$ species, but they decrease in parallel with their relative amounts approaching these limiting ratios. The derivations for the limiting ratios are given in the supplementary material along with a more complete discussion. (see paragraph at end of paper regarding supplementary material). The observed $^{18}O_3/^{18}O_2$ ratio is clearly below the limiting value (the arrow in Figure 1 indicates the limiting value for the $^{18}O_3$ species at 10 μM ADP based on the observed $^{18}O_2$ peak and the average enrichment in the P_i). Similar deviations have been observed in other experiments. The exchange, therefore, cannot be strictly explained by a simple random model. It should be emphasized that the presence of heterogeneous pathways for ATP synthesis cannot account for the deviations as heterogeneity produces deviations in the direction opposite to that observed.

Precision of Exchange Results. The low $^{18}O_3/^{18}O_2$ ratio observed in Figure 1 could be due to additional exchange with a low P_c value occurring subsequent to initial ATP synthesis. A limited amount of such exchange would cause partial conversion of the $^{18}O_3$ species into the $^{18}O_2$ species and a smaller conversion of $^{18}O_2$ into $^{18}O_1$ with a net result that the final $^{18}O_3/^{18}O_2$ ratio will be decreased below the initial value. Thus, it is important to establish that the observed distribution of isotopic species in 6PG is an accurate measure of the distribution in the ATP as initially release from the enzyme. This possibility was tested by performing a series of manipulations designed to mimic the experimental protocol of Figure 1, starting with a stock of ATP that was enriched with ^{18}O in the γ-position and whose starting $^{18}O_3/^{18}O_2$ ratio could be unambiguously assigned by ^{31}P NMR. The $^{18}O_3/^{18}O_2$ ratio of this initial ATP is given in line 1 of Table II. This ATP was reacted with hexokinase and glucose and then isolated and converted to 6PG. The $^{18}O_3/^{18}O_2$ ratio of the 6PG determined by ^{31}P NMR (line 2) was unchanged from that of the starting ATP, indicating that the reactions of hexokinase, glucose-6-phosphate dehydrogenase, and hydrolysis of the lactone of 6PG proceeded with no isotopic exchange. To test for any exchange that might occur during incubation of G6P in the reaction mix in the presence of submitochondrial particles, a complete reaction mix containing submitochondrial particles, hexokinase, 10 mM unenriched P_i, 0.02 mM ADP, and 1 mM [^{18}O]G6P obtained from the [^{18}O]ATP stock was incubated for 75 min and worked up as before. Analysis of the 6PG by ^{31}P NMR (line 3) indicated that the $^{18}O_0$ species was formed by ATP synthesis from the unenriched P_i, but the $^{18}O_3/^{18}O_2$ ratio of the enriched G6P remained unchanged.

Table II: Controls on Precision of ^{18}O Distributions

sample	$^{18}O_3/^{18}O_2$
(1) starting [γ-^{18}O]ATP	3.11
(2) [^{18}O]-6-phosphogluconate from [γ-^{18}O]ATP via hexokinase and glucose-6-phosphate dehydrogenase	2.99
(3) [^{18}O]-6-phosphogluconate from incubation of [^{18}O]glucose 6-phosphate with submitochondrial particles and workup as in line 2	3.12
(4) [β-^{18}O]ADP from [γ-^{18}O]ATP and AMP via adenylate kinase	2.87
(5) [^{18}O]-6-phosphogluconate from [β-^{18}O]ADP and submitochondrial particles via workup as in line 2	3.08

It is possible that the above controls do not adequately test for effects arising from the site of ATP synthesis being localized on the membrane of the submitochondrial particles. For example, ATP that is synthesized on the membrane may react with other membrane-bound enzymes, leading to further exchange before it can be converted to G6P by hexokinase in the bulk phase. In order to test for this possibility, the [^{18}O]ADP from line 4 of Table II was incubated with submitochondrial particles in the absence of added P_i and AMP, which results in ATP synthesis by the adenylate kinase that is bound to the submitochondrial particles.[2] The $^{18}O_3/^{18}O_2$ ratio in the 6PG produced from this reaction (line 5) is unchanged from that of the starting ATP (line 1), indicating that this extensive series of reactions was performed without exchange.

[2] Most of the mitochondrial adenylate kinase is located between the inner and outer membranes and is lost on formation of submitochondrial particles, but a fraction remains tightly bound to the submitochondrial particles and is not removed by repeated centrifugations. This bound adenylate kinase complicates the normal exchange analysis, and AMP or diadenosine pentaphosphate is usually included to inhibit it (Hackney & Boyer, 1978), but in this case it is used to advantage.

Table III: Theoretical Distributions for Nonequivalent and Square Model[a]

rates	distribution (%)			
	$^{18}O_0$	$^{18}O_1$	$^{18}O_2$	$^{18}O_3$
(1) nonequivalent: one tight subsite[b]				
1/1/1/1[c]	93.1	3.7	1.9	1.3
simple	93.1	3.7	1.9	1.3
1/16/1/1[c]	21.1	74.4	2.9	1.5
simple	53.1	20.8	14.5	11.6
1/20/1/1[c]	0	95.6	2.9	1.5
simple	43.0	23.5	18.1	15.4
(2) nonequivalent				
fast 2-fold rotation[d]	0.2	5.2	83.5	11.1
simple	8.7	19.0	30.2	42.1
(3) square				
center weighted[e]	59.9	24.0	11.5	4.6
simple	65.2	16.6	10.4	7.8
(4) square				
hyperheterogeneous[f]	83.3	0.14	1.7	14.8
simple	72.1	13.7	8.2	6.0

[a] All calculations are for a starting P_i enrichment of 100% and ATP synthesis in 0% [^{18}O]water. In each case, the distribution by a simple random model at the same average enrichment is included for comparison. See supplementary material for details. [b] Calculated for Scheme I with nonequivalent oxygens and additive subsite energies. Values for k_1P_i, k_{-1}, k_2, k_{-2}, k_3, k_{-3} and k_{ATP} were 10^4, 0, 10^3, 10^4, 10^2, 0, and 0 s^{-1}, respectively. [c] Subsite energies (kcal). [d] As in (1) with subsite energies of 6/6/6/6 kcal, except one 2-fold rotation was faster than predicted for a simple additive relationship. This rate for k_{AD} was 10^3 s^{-1}, and k_{-2} was 2×10^3 s^{-1}. [e] Calculated for Scheme II with k_1 = 100 s^{-1}, k'_1 = 0 s^{-1}, $k_2 = k_{-2} = k'_2 = k'_{-2}$ = 100 s^{-1}, k_3 = 0 s^{-1}, k'_3 = 20 s^{-1}, k_e = 0 s^{-1}, k_{-e} = 100 s^{-1}, $k_{-a} = k_{-p}$ = 0 s^{-1}, and $k_a = k_p$ = 10 s^{-1}. [f] Calculated for Scheme II with $k_1 = k_{-e} = k_2 = k_{-2} = k'_2 = k'_{-2} = k_3$ = 100 s^{-1}, $k_{-1} = k'_1 = k'_{-1} = k_{-3} = k'_{-3} = k_e = k_p = k_{-p} = k_{-a}$ = 0 s^{-1}, k'_3 = 0.001 s^{-1}, and k_a = 500 s^{-1}.

Theoretical Analysis of Nonequivalence. The deviations observed in Table I are unique in that they are center weighted with the $^{18}O_1$ and $^{18}O_2$ species overrespresented with respect to the simple random distribution at the same average enrichment. We have found two types of models that can produce center-weighted distributions of the type that is observed. One model involves nonequivalence of the P_i oxygen due to incomplete randomization of the oxygens during reversible synthesis of bound ATP. For example, if only one P_i oxygen was tightly bound to the enzyme active site, then the bound P_i could rotate around that bound oxygen and randomize the other three oxygens among themselves, resulting in their exchange, while the bound oxygen was inert to exchange. This would result in overrepresentation of the $^{18}O_1$ species in ATP synthesis starting from the $^{18}O_4$-labeled P_i species. Theoretical analysis of such nonequivalence is fairly simple for extreme cases of all-or-none scrambling (Hackney, 1980; Rosch, 1981) but is considerably more complex in the general case that is developed in detail in the supplementary material. This treatment of nonequivalence assumes that four subsites exist for binding each of the four P_i oxygens. Nonequivalence occurs when the subsites differ in binding energy (expressed as the activation energy for removal of an oxygen from each subsite), which will favor rotation of the bound P_i in certain directions over other directions. For example, the case with one tightly bound oxygen considered above would be modeled by assigning a binding energy to one subsite that is stronger than that for the other subsites.

Lines 1a–c of Table III indicate the influence of increased binding energy at one subsite modeled in this way. With only weak binding at all sites in line 1a, the P_i rotations are fast and the distributions is identical with that for the random model. With increasing interaction at only one site in lines 1b and 1c, however, the distributions become highly overrepresented in the $^{18}O_1$ species. Such a simple one-site model with one tight site is not fully able to account for the experimental distributions, however, as it cannot produce $^{18}O_3/^{18}O_2$ ratios less than 0.5 as seen here and developed more fully in the supplementary material. Lower $^{18}O_3/^{18}O_2$ ratios can be obtained if it is assumed that the rate of a rotation is not strictly dependent on the sum of the relevant subsite energies. Such a situation could be generated, for example, if two P_i oxygens were bound to a single arginine or lysine side chain in such a way that a 2-fold rotation about those two oxygens could occur via rotation about the single bonds of the amino acid side chains and would not require breaking the H bonds or other interactions linking the amino acids to the P_i oxygens. This produces distributions with the $^{18}O_2$ species overrepresented as indicated in line 2. Combination of these two types of nonequivalence in subsite binding energies can completely account for the observed deviations as indicated in Table I.

Scheme II

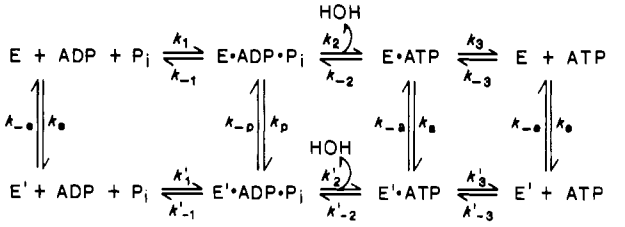

Theoretical Analysis of "Square" Model. The minimal model for a two-pathway reaction in Scheme II is usually invoked to account for heterogeneity when the interconversion between the two pathways is slow and the flux of ATP synthesis goes through each pathway independently. This yields end-weighted distributions if the pathways differ in R value defined as k_{-2}/k_3 or k'_{-2}/k'_3. Detailed analysis reveals, however, that square models of this type can also produce center-weighted distributions under a highly restrictive set of circumstances for the relative rates. This is indicated in line 3 of Table III[3] and developed in detail in the supplementary material. The key requirements are that the flux into the reaction scheme must be intially into a pathway with very slow product release such that most product release only occurs following transition to the other pathway (e.g., a transition between the pathways is forced to occur during each turnover). In this case, the main flux occurs into the top pathway, but product release cannot occur via step 3 and only can occur via step 3′ after transition to the lower pathway. Production of deviations additionally requires that k_{-2} and k'_3 cannot be fast with respect to the rate of transition between pathways and that k'_3 cannot be fast with respect to k'_{-2}.

These deviations result from the rapid loss of the $^{18}O_3$ species during the first few reversals of ATP synthesis as discussed above. Thus, several reversals of ATP synthesis occurs in the top pathway with preferential loss of the $^{18}O_3$ species before product release is possible via the lower pathway. In effect, there is a lag in the onset of product release during each turnover, and this biases the distribution of the released ATP against the $^{18}O_3$ species. This type of model can account for the observed deviations as indicated in Table I.

The converse situation of initial entry into a pathway with a significant product release rate followed by transition to a pathway with slow product release produces hyperheteroge-

[3] In assignment of rates to the square model, several rate constants are approximated as zero with the understanding that they are in fact finite and possess the appropriate relative magnitudes to satisfy the thermodynamic requirements of the internal cycles of the scheme.

Scheme III

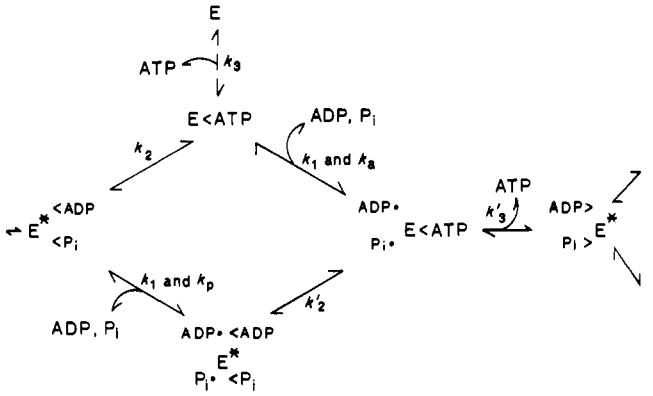

neous distributions that are more strongly end weighted than is possible for any linear combination of the two separate pathways. This is illustrated in line 4 for an entry pathway with a R value of 1 and an exit pathway with an R value of 10^5 with rapid and irreversible transition between pathways. An R value of 1 predicts an $^{18}O_3/^{18}O_2$ ratio of 2, and no larger ratio is possible by a linear combination with a second pathway of higher R value. This is in contrast to the $^{18}O_3/^{18}O_2$ ratio of 87 observed in line 4, which can be fit to a simple two independent pathway model with 83.3% hydrolysis by one pathway with an R value of 0.125. This type of model may be of important in analysis of the myosin ATPase, which exhibits strongly end-weighted distributions.

Discussion

The distributions reported here for ATP synthesis at low ADP in oxidative phosphorylation represent the first deviations from a simple equivalent model for the exchange that are not due to heterogeneity. These deviations can be produced by models that possesses nonequivalence of the P_i oxygens during the exchange process and by models of the square type with two pathways. Other types of models may also be possible. These models represent interesting possible explanations, but it is not currently possible to rigorously decide between them. The slow rotational rates that would be required for a nonequivalent model in this case are in contrast to the other enzymes that do not exhibit deviations. Also, the highly restricted set of relative rates required for observation of deviations with the square model would seem to limit its applicability.

It is interesting to note, however, that the alternating site model (Kayalar et al., 1977; Hackney & Boyer, 1978) is of the general square type and can account for the deviations noted here as well as all of the other unusual exchange properties of ATP reactions in oxidative phosphorylation. The key feature of an alternating site model is that substrate binding at one active site in an oligomeric complex is used to facilitate product release at a second coupled active site. The correspondence between this and Scheme II is indicated in Scheme III for one-half of an alternating site cycle adapted from eq 1 of Hackney and Boyer (1978) and shown for illustration with a dimeric system.[4] The steps in Scheme III are labeled with the rate constants of Scheme II to which they correspond. In this model, ADP and P_i bind at one site and start to undergo reversible ATP synthesis in step 2, but product release is not possible (e.g., $k_o \simeq$ zero) until transition to the region of step 2′ by binding of a second ADP and P_i via k_a and k_p. Furthermore, the highly arbitrary and restrictive set of relative rates required for observation of deviations with a square model are exactly the relative rates expected for the alternating site model at low ADP. Thus, the requirement for all product release to occur from E′ in step 3′ while all substrate binding occurs to E in step 1 is a natural consequence of an alternating site scheme in which each site cycles sequentially between E and E′. The binding change component of such model accounts for the low rate of product release via k_3 vs. k'_3. As developed in the supplementary material, deviations are only observed with a square model at low relative values of k_a and k_p. This feature of the model accounts for the observation of deviations at low ADP, but not at high ADP (Hackney, 1984), as the net k_a and k_p values are a function of the ADP level in Scheme III, being fast at high ADP and slow at low ADP. The dependence of the net ATP release rate on the ADP level (via k_a and k_p) also accounts for the increased overall level of exchange at low ADP with the system trapped in the region of step 2 as developed previously (Hackney & Boyer, 1978). The R value for exchange during ATP synthesis at saturating ADP and P_i is approximately 10 (Hackney & Boyer, 1978), which is consistent with $k'_{-2} < k'_3$ as required for observation of deviations. In contrast, during ATP hydrolysis the R value at saturating ATP is close to zero, which would account for the lack of observed deviations during hydrolysis even at low ATP.

[4] A three-site system is currently favored and would provide additional degrees of freedom, but a minimal two-site system is sufficient to produce the observed deviations. Any two-site model is a subset of a more general three-site model with the reactions at one site being fast with respect to the reactions at the other two sites.

Acknowledgments

We thank Dr. Chien Ho for access to NMR facilities and Virgil Simplaceanu for technical NMR support.

Supplementary Material Available

Analysis of limiting ratios at high exchange, theoretical analysis of nonequivalent oxygens, analysis of specific types of nonequivalence, kinetic isotope effects, fit to experimental data, and theoretical analysis of square model (17 pages). Ordering information is given on any current masthead page.

Registry No. ATP, 56-65-5; P_i, 14265-44-2; O, 7782-44-7.

References

Geeves, M. A., Webb, M. R., Midelfort, C. F., & Trentham, D. R. (1980) *Biochemistry 19*, 4748–4754.
Hackney, D. D. (1980) *J. Biol. Chem. 255*, 5320–5328.
Hackney, D. D. (1982) *J. Biol. Chem. 257*, 9494–9500.
Hackney, D. D. (1983) *Fed. Proc., Fed. Am. Soc. Exp. Biol. 42*, 1923a.
Hackney, D. D. (1984) *Curr. Top. Cell. Regul. 24*, 379–386.
Hackney, D. D., & Boyer, P. D. (1978) *J. Biol. Chem. 253*, 3164–3170.
Hackney, D. D., Rosen, G., & Boyer, P. D. (1979) *Proc. Natl. Acad. Sci. U.S.A. 76*, 3646–3650.
Hackney, D. D., Stempel, K. E., & Boyer, P. D. (1980) *Methods Enzymol. 64*, 60–83.
Hutton, R. L., & Boyer, P. D. (1979) *J. Biol. Chem. 254*, 9990–9993.
Kayalar, C., Rosing, J., & Boyer, P. D. (1977) *J. Biol. Chem. 252*, 2486–2491.
Midelfort, C. F. (1981) *Proc. Natl. Acad. Sci. U.S.A. 78*, 2067–2071.
Mitchell, R. A. (1984) *Curr. Top. Bioenerg. 13*, 203–255.
Mitchell, R. A., Lamos, C. M., & Russo, J. A. (1980) *Biochim. Biophys. Acta 592*, 406–414.

Rosch, P. (1981) *Z. Naturforsch., C: Biosci. 36C*, 539–544.
Rose, I. A. (1979) *Adv. Enzymol. Relat. Areas Mol. Biol. 50*, 361–395.
Shukla, K. K., & Levy, H. M. (1977a) *Biochemistry 16*, 132–136.
Shukla, K. K., & Levy, H. M. (1977b) *Biochemistry 16*, 5199–5206.
Shukla, K. K., Levy, H. M., Ramirez, F., Maracek, J. F., Meyerson, S., & Kuhn, E. S. (1980) *J. Biol. Chem. 255*, 11344–11350.
Sleep, J. A., Hackney, D. D., & Boyer, P. D. (1980) *J. Biol. Chem. 255*, 4094–4099.
Webb, M. R., & Trentham, D. R. (1980) *J. Biol. Chem. 255*, 8629–8632.
Wimmer, M. J., & Rose, I. A. (1977) *J. Biol. Chem. 252*, 6769–6775.

Interaction of Retinal Transducin with Guanosine Triphosphate Analogues: Specificity of the γ-Phosphate Binding Region†

Gregory Yamanaka,‡,§ Fritz Eckstein,‖ and Lubert Stryer*,‡

Department of Cell Biology, Sherman Fairchild Center, Stanford University School of Medicine, Stanford, California 94305, and Abteilung Chemie, Max-Planck-Institut für Experimentelle Medizin, D-3400 Göttingen, West Germany

Received February 27, 1986; Revised Manuscript Received May 7, 1986

ABSTRACT: The interaction of six hydrolysis-resistant analogues of GTP with transducin, the signal-coupling protein in vertebrate photoreceptors, was investigated. GppNHp and $GppCH_2p$ differ from GTP at the bridging position between the β- and γ-phosphate groups. The other analogues studied (GTPγF, GTPγOMe, GTPγOPh, and GTPγS) differ from GTP in containing a substituent on the γ-phosphorus atom or at a nonbridging γ-oxygen atom. Competition binding experiments were carried out by adding an analogue, [α-^{32}P]GTP, and a catalytic amount of photoexcited rhodopsin (R*) to transducin and measuring the amount of bound [γ-^{32}P]GTP. The order of effectiveness of these analogues in binding to transducin was

GTPγS > GTP ≫ GppNHp > GTPγOPh > GTPγOMe > $GppCH_2p$ > GTPγF

A second assay measured the effectiveness of GTPγS, GppNHp, and $GppCH_2p$ in eluting transducin from disc membranes containing R*. The basis of this assay is that transducin is released from disc membranes when it is activated to the GTP form. The relative potency of these three analogues in converting transducin from a membrane-bound to a soluble form was 1000, 75, and 1, respectively. Stimulation of cGMP phosphodiesterase activity served as a third criterion of the interaction of these analogues with transducin. The order of effectiveness of these analogues in promoting the transducin-mediated activation of the phosphodiesterase was

GTPγS > GTP ≫ GppNHp > GTPγOPh ≫ $GppCH_2p$ > GTPγOMe > GTPγF

GTPγS was more than a 1000 times as potent as GTPγF in activating the phosphodiesterase. For GTPγOPh, GTPγOMe, and GTPγF, the order of effectiveness in stimulating the phosphodiesterase was the same as previously reported for the activation of adenylate cyclase in pigeon erythrocyte membranes [Pfeuffer, T., & Eckstein, F. (1976) *FEBS Lett. 67*, 354–358] but the opposite of that found with bacterial elongation factor G [Eckstein, F., Bruns, W., & Parmeggiani, A. (1975) *Biochemistry 14*, 5225–5232]. Thus, transducin and the stimulatory G protein have similar binding sites for the γ-phosphoryl group of GTP, whereas that of elongation factor G is significantly different.

The photoexcitation of rhodopsin in vertebrate retinal rod outer segments (ROS)[1] triggers a cascade that results in the hydrolysis of many molecules of cGMP (Miller, 1981; Chabre, 1985; Stryer, 1986). Transducin, a multisubunit peripheral membrane protein, is the information carrier in the activation of the cyclic GMP phosphodiesterase (PDE) (Fung et al., 1981). Transducin consists of a 39-kDa α chain that binds guanyl nucleotides, a 36-kDa β chain, and an 8-kDa γ chain (Kühn, 1980). In the dark, transducin is bound to the disc membrane in the GDP form (T–GDP). Photoexcited rhodopsin (R*) catalyzes the exchange of GTP for GDP bound to the α subunit (Godschaux & Zimmerman, 1979). About 500 molecules of T_α–GTP are formed per R* at low light levels

† This research was supported by grants from the National Eye Institute and the National Institute of General Medical Sciences. G.Y. is a Fellow of the Jane Coffin Childs Memorial Fund for Medical Research.
‡ Stanford University School of Medicine.
§ Present address: Virus & Cell Biology, Merck Sharp & Dohme Research Laboratories, West Point, PA 19486.
‖ Max-Planck-Institut für Experimentelle Medizin.

[1] Abbreviations: ROS, rod outer segment; T, transducin; PDE, cGMP phosphodiesterase; R*, urea-stripped disc membranes containing photolyzed rhodopsin; DTT, dithiothreitol; GppNHp, guanosine 5′-(β,γ-imidotriphosphate); $GppCH_2p$, guanosine 5′-(β,γ-methylenetriphosphate); GTPαS, guanosine 5′-*O*-(1-thiotriphosphate); GTPβS, guanosine 5′-*O*-(2-thiotriphosphate); GTPγS, guanosine 5′-*O*-(3-thiotriphosphate); GTPγF, guanosine 5′-*O*-(3-fluorotriphosphate); GTPγOMe, guanosine 5′-*O*-(3-methyl triphosphate); GTPγOPh, guanosine 5′-*O*-(3-phenyl triphosphate); EF-G, elongation factor G; EF-Tu, elongation factor Tu; Tris-HCl, tris(hydroxymethyl)aminomethane hydrochloride; SDS, sodium dodecyl sulfate.

0006-2960/86/0425-6149$01.50/0